

STABILITY ANALYSIS OF A SPINNING SHAFT IN THE CONCENTRIC CYLINDER FILLED WITH AN INCOMPRESSIBLE FLUID

ZHONGKAI JIANG, GUANGDING WANG

*School of Engineering, Anhui Agricultural University, Hefei, China; and
Anhui Province Engineering Laboratory of Intelligent Agricultural Machinery and Equipment, Hefei, China
e-mail: ahau_evib@163.com; wgd_vib@yeah.net*

HUIQUN YUAN

*Institute of Applied Mechanics, College of Science, Northeastern University, Shenyang, China
e-mail: hq_yuan@yeah.net*

This paper deals with the stability of a spinning shaft in a concentric cylinder filled with an incompressible fluid. The steady-state momentum and continuity equations for the external fluid are established. Using Taylor expansion, the fluid forces exerted on the shaft are calculated. The shaft is in the Rayleigh model taking into account the rotary inertia and gyroscopic effects. Accordingly, the governing equation of the considered system is formulated analytically. The explicit characteristic frequency equation for the pinned-pinned spinning shaft system is then derived. Finally, the stability of the system is studied by means of characteristic value analysis.

Keywords: spinning shaft, external fluid, stability, critical spinning speed

1. Introduction

Spinning shafts have held wide applications in energy, aviation and automotive engineering. One class of spinning shafts works in an annular fluid medium, such as the spinning shaft of axial flow pumps. In the large pump unit, its hydraulic components are subject to various hydraulic unbalanced forces and other various excitation sources during the operation of the unit. As a result, vibration and instability of the structure occur, which will directly affect the reliable operation of the unit. In this study, a spinning shaft in a concentric cylinder filled with an incompressible fluid is considered. The focus is on the instability characteristics of the spinning shaft with external fluids.

The vibration and stability of spinning shafts are key concerns in engineering, which have attracted attention of many researchers. There are two analytical methods for such problems, one is the analytical study and the other is numerical calculation (Chen and Ku, 1990; Gross *et al.*, 1993). Sheu and Yang (2005) conducted an analytical study of vibration for a rotating Rayleigh beam with typical boundary conditions as well as an analysis of the unbalanced response. Using the Hamilton principle and multiple scales method, natural vibration of a nonlinear slender spinning shaft was investigated by Shahgholi *et al.* (2014). Zhang *et al.* (2020a) studied the frequency and mode of a flexible rotor system using Hamilton's principle and Euler's angle, and discussed the effect of centrifugal forces on the stability of the system. In recent years, researchers have been concerned with vibration of shafts under simultaneous effects of axial movement and rotational motion (Zhu and Chung, 2019; Ebrahimi-Mamaghani *et al.*, 2021; Yang *et al.*, 2021; Li *et al.*, 2018; Katz, 2001). For example, applying the Hamilton principle, Zhu and Chung (2019) derived the governing equation of motion for a simply supported Rayleigh beam with spinning and axial

motions. Using the Galerkin method, vibration and stability of the beam were studied. Ebrahimi-Mamaghani *et al.* (2021) considered the effects of spinning and axial motions and investigated stability of an axially functionally graded beam via the Laplace transform and Galerkin discretization. In summary, there is a great deal of literature reporting on the dynamics and stability of spinning shafts, and the study in this area has been relatively extensive (Aouadi and Lakrad, 2018; Arvin, 2019; Saeed, 2019; Manchi and Sujatha, 2021; Li, 2022; Li *et al.*, 2021; Zhu *et al.*, 2018).

Furthermore, there are many studies concerning fluid-structure coupled vibration of spinning shafts, such as liquid-filled rotors and spinning pipes conveying fluids. For the liquid-filled rotor, the flexural vibration governing equation of the rotor is established by the analytical calculation method, and the characteristic frequency equation of the system is derived by combining the corresponding support boundary conditions. Then, the stability of the rotor system is analyzed by the positive and negative signs of the characteristic roots (Tao and Zhang, 2002; Firouz-Abadi and Haddadpour, 2010; Kern and Jehle, 2016; Sahebnasagh *et al.*, 2018; Wang and Yuan, 2018; Wang and Yuan, 2019b; Wang and Chen, 2020; Wang *et al.*, 2021; Zhang *et al.*, 2020b; Wang and Yuan, 2021; Païdoussis and Issid, 1974). Commonly, the two-dimensional linearized Navier-Stokes equation is employed to calculate the fluid forces on the rotor (Tao and Zhang, 2002; Firouz-Abadi and Haddadpour, 2010; Wang and Chen, 2020). Wang and Yuan (2018) established three-dimensional equations of fluid motion in the rotor cavity and studied stability of the rotor system. In addition to the above-mentioned stability discrimination methods, Wang and Chen (2020; 2021) also applied the Andronov-Hopf bifurcation and wave resonance theory to investigate stability of the fluid-filled rotor system. On the other hand, many advanced papers have reported vibration and stability of spinning pipes conveying fluid in literature on the study (Abdollahi *et al.*, 2021; Dwivedi *et al.*, 2022; Michaelides and Feng, 2023; Wang and Yuan, 2019a; Oyelade and Oyedirin, 2020). Basically, the spinning pipe is seen as a beam structure. The structural equations of motion are established based on the Euler-Bernoulli beam or Rayleigh beam theory (Païdoussis and Issid, 1974; Kheiri *et al.*, 2014). In terms of solution methods, numerical calculation methods are more frequently used, such as the transfer matrix method (Li *et al.*, 2014), Galerkin method (Bahaadini *et al.*, 2018; Liang *et al.*, 2018; Liang *et al.*, 2020), and the differential quadrature method (DQM) (Zhou *et al.*, 2018). There are also some studies reporting vibration of spinning pipes conveying fluid under external loads including additional mass (ElNajjar and Daneshmand, 2020), thermal effects (Qian *et al.*, 2009; Bahaadini and Saidi, 2018), etc. It can be found that the studies on the vibration of spinning pipes conveying fluid are basically consistent in terms of research methods. In general, theoretical studies on fluid-structure coupled vibration of spinning cylinders/pipes are common. However, there are few reports on vibration and stability of spinning shafts in an annular fluid medium.

In summary, most of the studies have investigated vibration of spinning shafts subjected to external loads. Also, some studies have reported instability of pipes conveying fluid. On the other hand, there was very little literature studying the vibration of shafts with external fluids. The present paper is aimed to investigate the instability of a spinning slender shaft in a concentric cylinder filled with an incompressible fluid. Accordingly, the rotary inertia and gyroscopic effects are considered in the modeling of the considered system. The steady-state governing equations of fluid motion are established, and the external fluid forces are obtained by means of Taylor expansion. Then the coupled-field governing equations of the shaft and external fluid are derived on the basis of the spinning Rayleigh beam theory. After that, the characteristic frequency equation of the system is determined and then used for stability analysis. Finally, the effects of the slenderness ratio and density ratio on the natural frequency, instability and critical spinning speed are studied numerically.

2. Fluid dynamics

2.1. Formulation for the external fluid

Consider a spinning shaft in a concentric cylinder filled with an incompressible fluid as shown in Fig. 1. It has rotational speed Ω , length of shaft L , radius of cylinder a , fluid density ρ_f , and b refers to the radius of the shaft. It is assumed that the shaft spins at a steady state. Since perturbations due to flexural deformation of the shaft occur, vibrational instability of the shaft will be generated as a result of the perturbed pressure P formed by the external fluid. In order to reveal the instability characteristics of the spinning shaft, this subsection will be devoted to the formulation of the external fluid force.

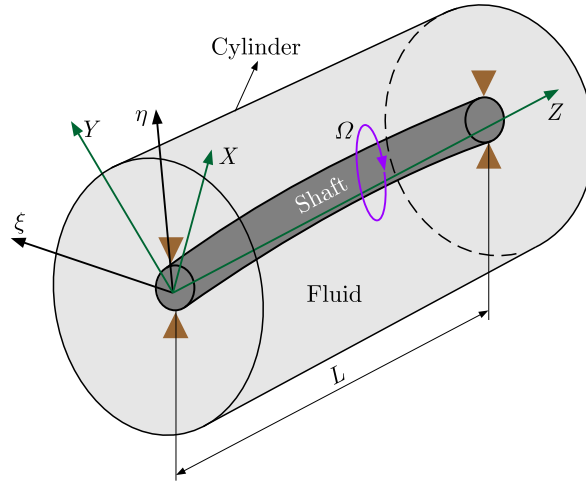


Fig. 1. Schematic of a spinning shaft in the concentric cylinder filled with an incompressible fluid

In the steady state, the two-dimensional Navier-Stokes equations and continuity equation of the external fluid in the rotating frame $\eta\xi$ can be written as

$$\begin{aligned} -2\Omega v_\theta - r\Omega^2 + v_r \frac{\partial v_r}{\partial r} + \frac{v_\theta}{r} \frac{\partial v_r}{\partial \theta} - \frac{v_\theta^2}{r} &= -\frac{1}{\rho_f} \frac{\partial P}{\partial r} + \nu \left(\nabla^2 v_r - \frac{v_r}{r^2} - \frac{2}{r^2} \frac{\partial v_\theta}{\partial \theta} \right) \\ 2\Omega v_r + v_r \frac{\partial v_\theta}{\partial r} + \frac{v_\theta}{r} \frac{\partial v_\theta}{\partial \theta} + \frac{v_r v_\theta}{r} &= -\frac{1}{\rho_f r} \frac{\partial P}{\partial \theta} + \nu \left(\nabla^2 v_\theta - \frac{v_\theta}{r^2} + \frac{2}{r^2} \frac{\partial v_r}{\partial \theta} \right) \end{aligned} \quad (2.1)$$

and

$$\frac{\partial(rv_r)}{\partial r} + \frac{\partial v_\theta}{\partial \theta} = 0 \quad (2.2)$$

where v_r and v_θ denote the radial and tangential velocity components of fluid particles, respectively, and ν is kinematic viscosity. Also, ∇^2 is the Laplacian operator which is defined as

$$\nabla^2 = \frac{\partial^2}{\partial r^2} + \frac{1}{r} \frac{\partial}{\partial r} + \frac{1}{r^2} \frac{\partial^2}{\partial \theta^2} \quad (2.3)$$

The corresponding flow boundary conditions at $r = a, b$ are

$$\begin{aligned} v_r \Big|_{r=b} &= 0 & v_\theta \Big|_{r=b} &= b\Omega \\ v_r \Big|_{r=a} &= 0 & v_\theta \Big|_{r=a} &= 0 \end{aligned} \quad (2.4)$$

According to the proposed model, it is noticed that in this flow, the circumferential velocity is valued, but the derivative of all parameters along the circumference is equal to zero, i.e. $\partial/\partial\theta = 0$. Moreover, under the boundary conditions given in Eqs. (2.4), the continuity equation shown in Eq. (2.2) is solved to obtain the radial velocity component $v_r = 0$. By substituting these conditions into Eqs. (2.1), we get

$$2\Omega v_\theta - r\Omega^2 - \frac{v_\theta^2}{r} = -\frac{1}{\rho_f} \frac{\partial P}{\partial r} \quad \frac{1}{r} \frac{\partial}{\partial r} \left(r \frac{\partial v_\theta}{\partial r} \right) - \frac{v_\theta}{r^2} = 0 \quad (2.5)$$

By solving Eq. (2.5)₂, the solution of the circumferential velocity component v_θ can be obtained as

$$v_\theta = Ar + \frac{B}{r} \quad (2.6)$$

where

$$A = \frac{\Omega}{1 - \kappa^2} \quad B = \frac{a^2 \Omega}{\kappa^2 - 1} \quad (2.7)$$

in which κ is defined as

$$\kappa = \frac{a}{b} \quad (2.8)$$

Since v_θ is determined, the total pressure P can be calculated in terms of Eq. (2.5)₁ as

$$P = \rho_f \Omega^2 \left(\frac{1}{2} r^2 + \chi r^2 - \frac{a^4 \chi^2}{2r^2} + \frac{1}{2} r^2 \chi^2 - 2a^2 \chi \ln r - 2a^2 \chi^2 \ln r \right) + C \quad (2.9)$$

where

$$\chi = \frac{1}{1 - \kappa^2} \quad (2.10)$$

Due to the influence of flexural deformation of the spinning shaft, the fluid particles on the surface of the shaft will undergo in a corresponding radial displacement. Assuming that the radial displacement is ζ , substituting into Eq. (2.9) yields

$$P|_{b+\zeta} = \rho_f \Omega^2 \left[\frac{1}{2} (b+\zeta)^2 + \chi (b+\zeta)^2 - \frac{a^4 \chi^2}{2(b+\zeta)^2} + \frac{1}{2} (b+\zeta)^2 \chi^2 - 2a^2 \chi \ln(b+\zeta) - 2a^2 \chi^2 \ln(b+\zeta) \right] + C \quad (2.11)$$

As seen, Eq. (2.11) is a nonlinear expression. As a result, the Taylor expansion is employed to linearize this equation. The linearization expression for the pressure P can be expressed as

$$P = \rho_f \Omega^2 \left[\frac{1}{2} b^2 + \chi b^2 - \frac{a^4 \chi^2}{2b^2} + \frac{1}{2} b^2 \chi^2 - 2a^2 \chi \ln b - 2a^2 \chi^2 \ln b \right] \\ + \rho_f \Omega^2 b \zeta \left[(1 + \chi)^2 + \frac{a^4 \chi^2}{b^4} - \frac{2a^2 \chi}{b^2} - \frac{2a^2 \chi^2}{b^2} \right] + C \quad (2.12)$$

It can be found that the part of Eq. (2.12) containing ζ is a perturbed term caused by deformation of the spinning shaft, which is the main source of the instability. In this study, only the perturbation pressure needs to be concerned. Therefore, Eq. (2.12) can be simplified as

$$P = \rho_f \Omega^2 b [(1 + \chi) - \kappa^2 \chi]^2 \zeta \quad (2.13)$$

By substituting Eq. (2.10) into Eq. (2.13), the perturbed pressure acting on the surface of the spinning shaft can be determined as

$$P = 4\rho_f\Omega^2b\zeta \tag{2.14}$$

in which the radial displacement ζ can be described by the flexural deformation of the shaft as

$$\zeta = u_\eta \cos \theta + u_\xi \sin \theta \tag{2.15}$$

where u_η and u_ξ are displacement components of the spinning shaft in the η and ξ directions, respectively.

Finally, the fluid forces exerted on the shaft can be calculated as

$$F_\eta = \int_0^{2\pi} P(b) \cos(\theta)b \, d\theta \qquad F_\xi = \int_0^{2\pi} P(b) \sin(\theta)b \, d\theta \tag{2.16}$$

After substituting Eqs. (2.14) and (2.15) into Eqs. (2.16), the analytical expressions for the fluid forces can be obtained as

$$F_\eta = 4\rho_f\pi b^2\Omega^2u_\eta \qquad F_\xi = 4\rho_f\pi b^2\Omega^2u_\xi \tag{2.17}$$

3. Structural dynamics

In this study, the rotary inertia and gyroscopic effects of the spinning shaft are both considered. Therefore, the Rayleigh model is adopted to formulate the governing equation of motion of the spinning shaft in the concentric cylinder filled with an incompressible fluid.

If adopting the Rayleigh beam theory, the basic governing differential equation for flexural vibration of the considered spinning shaft system reads

$$EI \frac{\partial^4 u}{\partial Z^4} + \rho A \frac{\partial^2 u}{\partial t^2} - \rho I \frac{\partial^4 u}{\partial t^2 \partial Z^2} + i2\rho I \Omega \frac{\partial^3 u}{\partial t \partial Z^2} = F \tag{3.1}$$

where E , I , A and ρ are Young's modulus, mass moment of inertia, cross-sectional area and density of the shaft, respectively. Also, the fluid force F can be obtained by using Eqs. (2.17) as

$$F = 4\rho_f\pi b^2\Omega^2u \tag{3.2}$$

where flexural deformation u is defined as

$$u = u_\eta + iu_\xi \tag{3.3}$$

After inserting Eq. (3.2) into Eq. (3.1), the governing equation can be rewritten as

$$EIu'''' + \rho A\ddot{u} - \rho I\ddot{u}'' + i2\rho I\Omega\dot{u}'' = 4m_f\Omega^2u \tag{3.4}$$

where m_f is defined as $m_f = \rho_f\pi b^2$.

Since only harmonic vibrations are considered, $u(Z, t)$ may take the form as

$$u(Z, t) = U(Z)e^{i\omega t} \tag{3.5}$$

where ω is the circular frequency of vibration of the spinning shaft.

After using the above expression for u in Eq. (3.5) into Eq. (3.4), one gets

$$EIU'''' + (\rho I\omega^2 - 2\rho I\Omega\omega)U'' - (\rho A\omega^2 + 4m_f\Omega^2)U = 0 \tag{3.6}$$

To simplify the analysis, the following dimensionless quantities are introduced

$$\varsigma = \frac{Z}{l} \quad W = \frac{U}{l} \quad \gamma = \frac{l}{r} \quad \omega_0^2 = \frac{EI}{\rho Al^4} \quad g = \frac{\omega}{\omega_0} \quad s = \frac{\Omega}{\omega_0} \quad (3.7)$$

Then, the dimensionless form of Eq. (3.6) can be written as

$$W'''' + \left[\left(\frac{1}{2\gamma} \right)^2 g^2 - 2 \left(\frac{1}{2\gamma} \right)^2 gs \right] W'' - (g^2 + 4\mu s^2) W = 0 \quad (3.8)$$

where density ratio μ is given as

$$\mu = \frac{\rho f}{\rho} \quad (3.9)$$

It is well known that the general form of the solution to Eq. (3.8) can be expressed as

$$W(\varsigma) = C_1 \sin(\alpha\varsigma) + C_2 \cos(\alpha\varsigma) + C_3 \sinh(\beta\varsigma) + C_4 \cosh(\beta\varsigma) \quad (3.10)$$

Considering that the two ends of the spinning shaft are hinged in this study, the corresponding dimensionless boundary conditions at $\varsigma = 0$ and 1 are

$$W \Big|_{\varsigma=0} = W \Big|_{\varsigma=1} = 0 \quad W'' \Big|_{\varsigma=0} = W'' \Big|_{\varsigma=1} = 0 \quad (3.11)$$

Using Eq. (3.11), the characteristic frequency equation of the spinning shaft can be obtained as

$$\sin \alpha = \sin(n\pi) \quad (3.12)$$

where α can be determined by using Eqs. (3.8) and (3.10).

After expanding Eq. (3.12), the explicit expression of the dimensionless characteristic frequency equation is expressed as

$$n^4 \pi^4 - n^2 \pi^2 (g^2 - 2gs) \left(\frac{1}{2\gamma} \right)^2 - (g^2 + 4\mu s^2) = 0 \quad (3.13)$$

It can be seen that the characteristic equation is an algebraic equation with respect to the dimensionless whirl frequency g . Solving this equation, the real and imaginary parts of the eigenvalues can be determined, i.e. $g = \lambda + i\sigma$, where the real part represents the dimensionless natural frequency of the system and the imaginary part represents the dimensionless damping. Also, the stability of the system can be determined by the variation of the real and imaginary parts versus the dimensionless spinning frequency (Abdollahi *et al.*, 2021). In the present study, it is supposed that both ends of the shaft are pinned-pinned boundary conditions. Therefore, the other boundary conditions are not included in the mathematical formulation. However, the method described in this article is also applicable to examine stability of spinning shafts in the concentric fluid-filled cylinder with other boundary conditions.

Furthermore, by inserting $g = s$ into Eq. (3.13), the dimensionless critical spinning speed can be calculated as

$$s_n^c = n^2 \pi^2 \sqrt{\frac{1}{1 + 4\mu - n^2 \pi^2 \left(\frac{1}{2\gamma} \right)^2}} \quad (3.14)$$

As seen, if supposing $\gamma = 0$, then the critical spinning speed can be reduced to

$$s_n^c = n^2 \pi^2 \sqrt{\frac{1}{1 - n^2 \pi^2 \left(\frac{1}{2\gamma} \right)^2}} \quad (3.15)$$

which is identical to that for pinned-pinned spinning Rayleigh beams (Sheu and Yang, 2005).

4. Numerical results

In this Section, a numerical study is conducted to investigate the instability of the spinning shaft in the concentric cylinder filled with an incompressible fluid. In particular, the factors that affect the stability of the system are discussed in depth.

In order to validate the proposed model, the first four critical spinning speeds versus slenderness ratio for the spinning Rayleigh beams without the external fluid are obtained and compared with those reported by Sheu and Yang (2005), as shown in Fig. 2. It can be seen that the present results are in good agreement with those obtained in the literature. Furthermore, to clarify the effect of the external fluid, the critical spinning speeds of the spinning shaft with the external fluid are illustrated and compared with the spinning shaft without considering external fluid effects, as seen in Fig. 3. It can be observed that after considering the external fluid, the critical spinning speed for each order has become noticeably smaller.

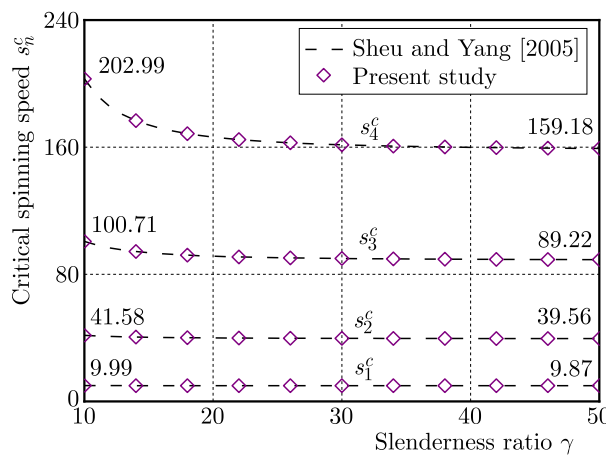


Fig. 2. Comparison of the first four critical spinning speeds versus slenderness ratio of the spinning shaft with Sheu and Yang (2005) at $\mu = 0$

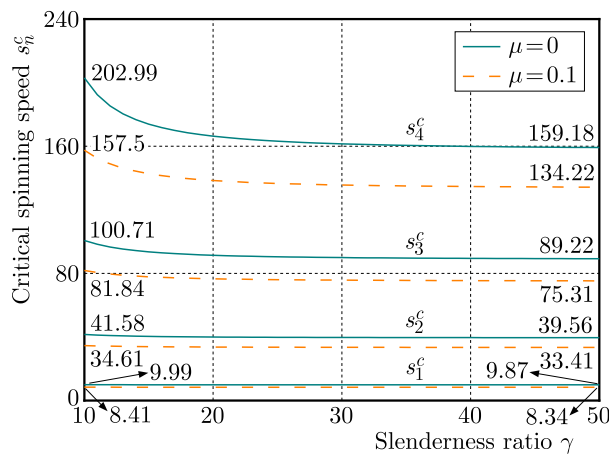


Fig. 3. The effects of external fluid on the critical spinning speed of the spinning shaft

Figure 4 shows the whirl speed map of the spinning shaft in the concentric cylinder filled with the incompressible fluid for $\mu = 0.13$, $\gamma = 5$ and different values of the mode number. Also, in order to clarify the influence of the external fluid on the spinning shaft, the whirl speed map of the spinning Rayleigh beam is plotted in the figure. It can be seen that the critical spinning speed of the system decreases significantly at each order due to the influence of the external fluid. In addition, the dimensionless whirl frequency of the system no longer increases with the

dimensionless spinning frequency, but the two characteristic frequencies are converged at a point, forming a closed arc-shaped region. It indicates that the characteristic equation has no real roots when the spinning speed is higher than the speed at the convergence point. This result shows that the external fluid has a strong influence on the whirl characteristics and stability of the spinning shaft.

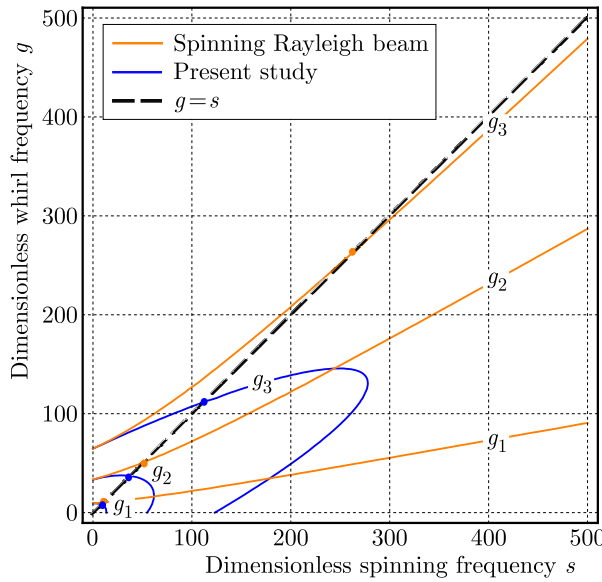


Fig. 4. Comparison of whirl speed maps of the spinning Rayleigh beam and the considered spinning shaft system

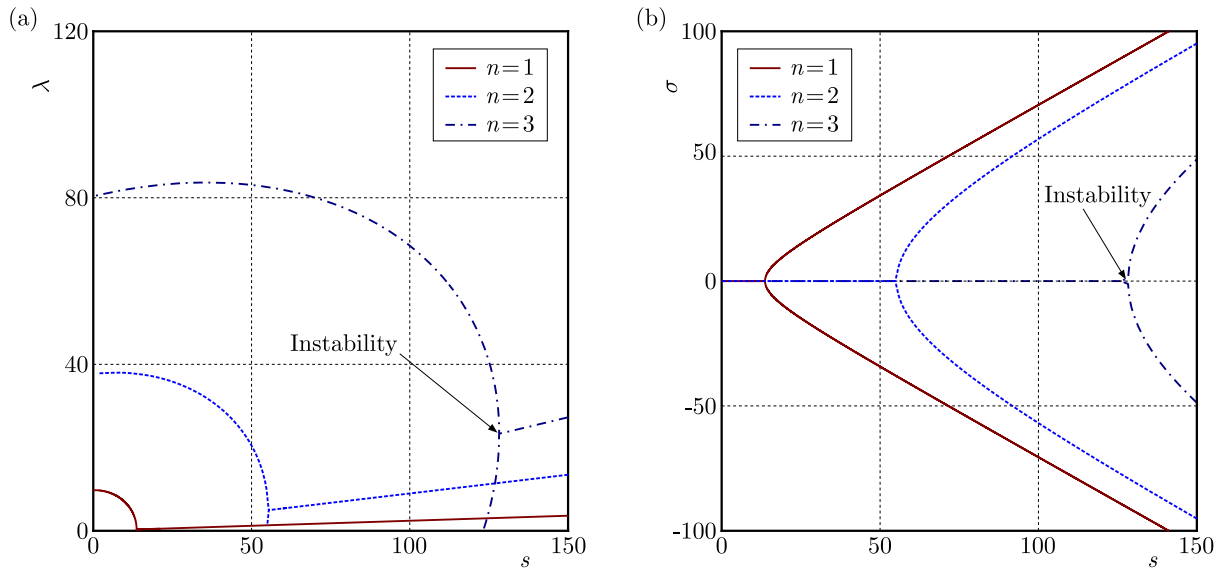


Fig. 5. Dimensionless natural frequency and damping of the spinning shaft versus the dimensionless spinning frequency with $\mu = 0.13$ and $\gamma = 10$ for different mode numbers: (a) dimensionless natural frequency, (b) dimensionless damping

Figures 5a and 5b, respectively, demonstrate the dimensionless natural frequency and damping of the system in terms of the dimensionless spinning frequency at $\mu = 0.13$ and $\gamma = 10$ for different mode numbers. It can be seen that as the spinning frequency increases, the natural frequency of the system for both modes decreases. The damping of the system bifurcates at a specific speed, which indicates that there is an inflow and outflow of energy and the system

becomes unstable. The speed corresponding to the bifurcation point is called the “instability critical spinning speed s_{cr} ”. Moreover, a comparative study is carried out to illustrate the effect of the external fluid on the stability of the considered system, as shown in Fig. 6. It can be found that the spinning Rayleigh beam is always stable as the rotational speed increases. However, when considering the external fluid, the system will lose its stability at a certain speed. This makes it clearer that external fluids are the main source of instability.

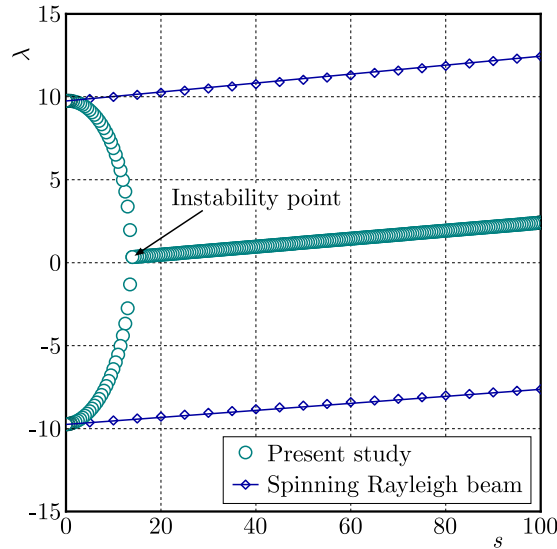


Fig. 6. Comparison of the dimensionless natural frequencies of the spinning shaft in the concentric cylinder filled with the incompressible fluid and spinning Rayleigh beams

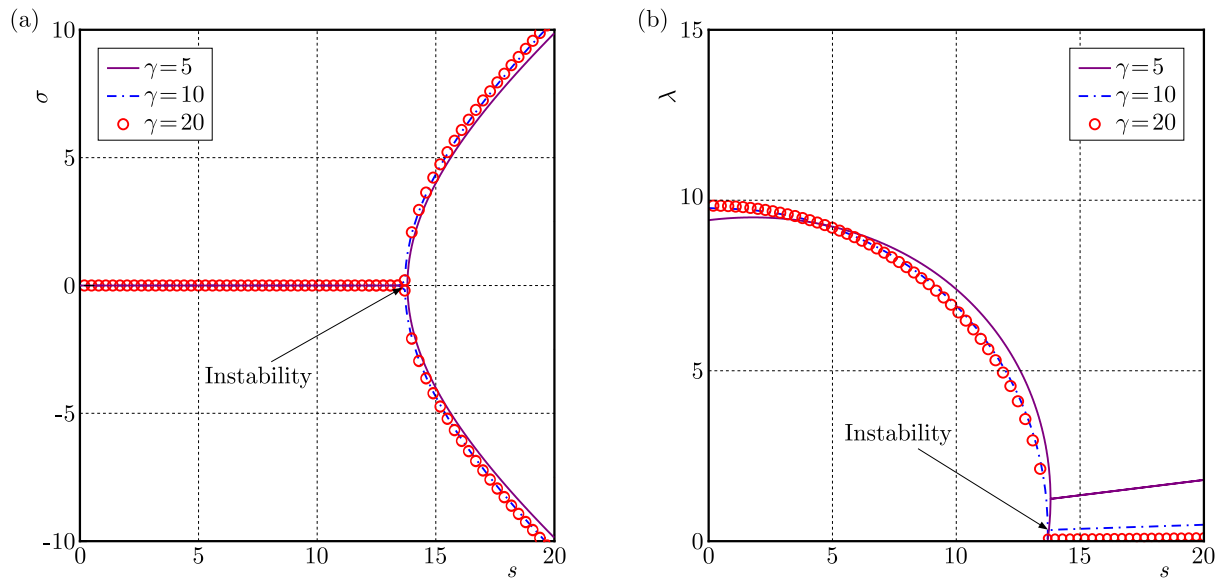


Fig. 7. Dimensionless natural frequency and damping for the spinning shaft versus the dimensionless spinning frequency with $n = 1$ and $\mu = 0.13$ for various values of the slenderness ratio: (a) dimensionless natural frequency, (b) dimensionless damping

Variations of the dimensionless natural frequency and damping of the system versus the dimensionless spinning speed at $n = 1$ and $\mu = 0.13$ for various values of the slenderness ratio are depicted in Fig. 7. It can be seen that for the first-order mode, the variation of the natural frequency of the system is not obvious with the increase of the slenderness ratio. Especially, when the value of the slenderness ratio is large ($\gamma \geq 10$), the natural frequency is generally

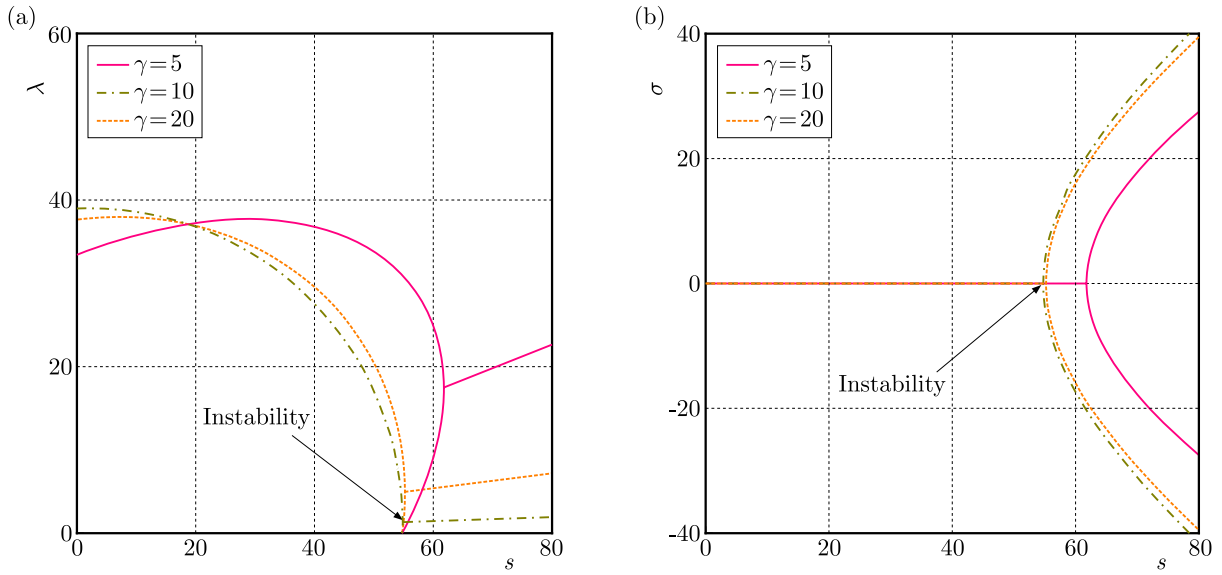


Fig. 8. Dimensionless natural frequency and damping of the spinning shaft versus the dimensionless spinning frequency with $n = 2$ and $\mu = 0.13$ for various values of the slenderness ratio: (a) dimensionless natural frequency, (b) dimensionless damping

consistent. It also can be seen in Fig. 7b that by increasing the slenderness ratio, the instability points are almost coincident. This means that the effect of slenderness ratio on the system instability can be negligible. However, it is interesting to note that for higher-order modes, the effect of the slenderness on the natural frequency and stability of the system is more pronounced. Figure 8 shows the dimensionless natural frequency and damping of the spinning shaft versus the dimensionless spinning frequency with $n = 2$ and $\mu = 0.13$ at different slenderness ratios. It can be found that as the slenderness ratio increases, the natural frequency of the system first increases and then decreases. At the same time, the instability critical spinning speed s_{cr} decreases. However, for large slenderness ratios ($\gamma \geq 10$), the variation of critical spinning speed is still not noticeable. This indicates that the smaller slenderness ratio leads to a greater effect on the stability of the system. Furthermore, the effects of the slenderness ratio on the unstable region of the considered spinning shaft system are reported in Fig. 9. Results show that the

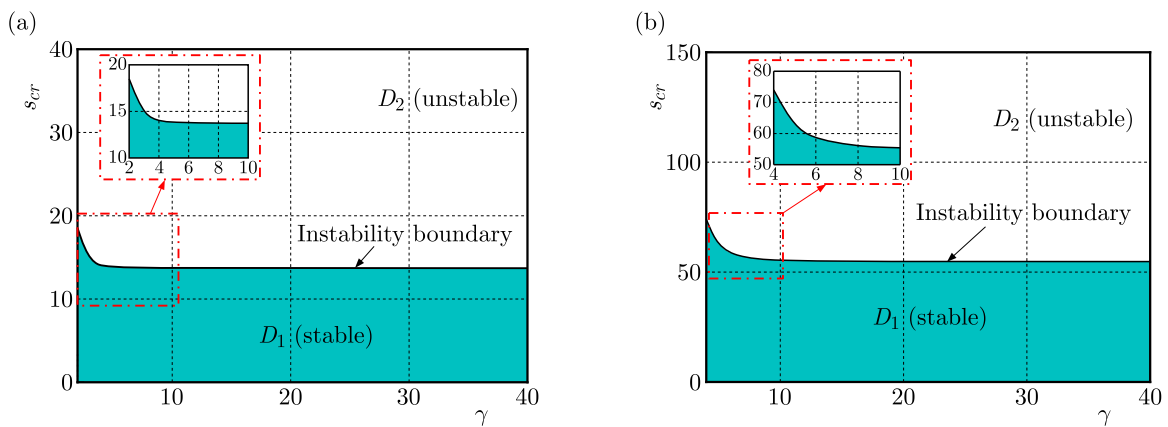


Fig. 9. Effects of the slenderness ratio γ on the instability of the spinning shaft system for different mode numbers: (a) $n = 1$, (b) $n = 2$

critical spinning speed experiences a smooth decrease and then converges to a constant value with an increase of the slenderness ratio. Also, the instability boundary is formed, and the whole speed domain is divided into two parts, D_1 and D_2 , where D_1 is the stable region and D_2 is

the unstable region. As shown in the subfigure of Fig. 9, the instability boundary only changes when the slenderness ratio is small enough for both the first and second modes. Therefore, it can be concluded that at higher slenderness ratios, say $\gamma > 10$, the effect of rotary inertia on the system stability can be negligible.

The dimensionless natural frequency and damping of the considered spinning shaft system versus the dimensionless spinning frequency for a variety of density ratios at $n = 1$ and $\gamma = 10$ are plotted in Fig. 10. Figure 10a demonstrates that a higher value of density ratio leads to a lower value of natural frequency. Also, it can be observed in Fig. 10b that as the density ratio increases, the instability critical spinning speeds are reduced. This means that for larger density ratios, the system is more prone to lose its stability. Figure 11 shows the effect of density ratio on the instability of the system. As can be seen, the instability boundary decreases with respect to the density ratio. The instability critical spinning speed gradually moves towards the low-speed region. The results indicate that the density of the external fluid plays a dominant role in the stability of the shaft system.

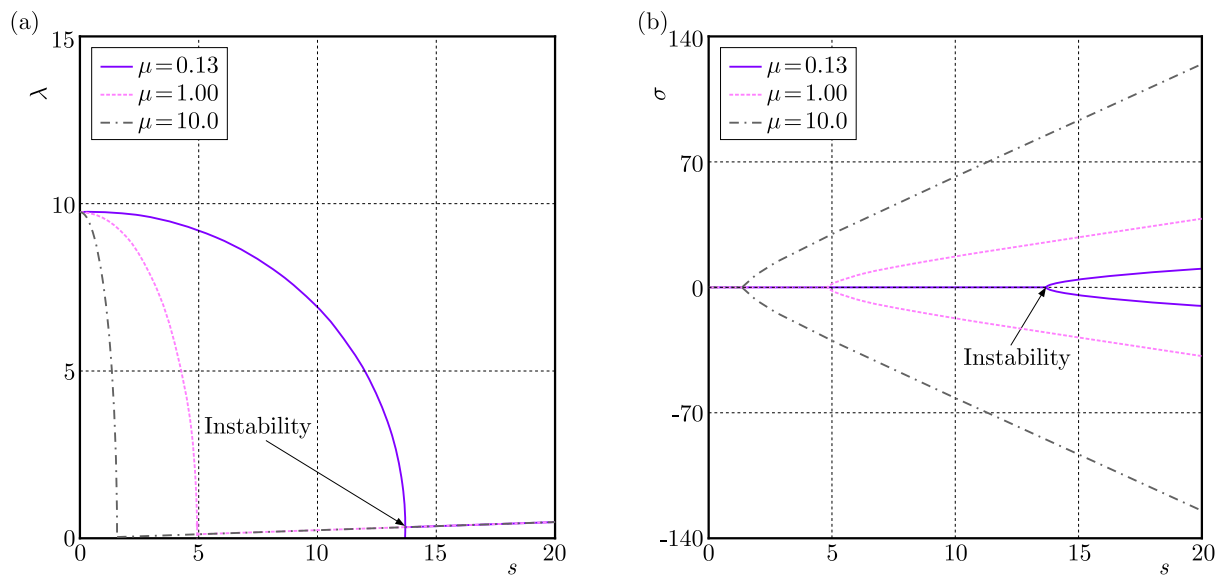


Fig. 10. Dimensionless natural frequency and damping of the spinning shaft versus the dimensionless spinning frequency with $n = 1$ and $\gamma = 10$ for various values of the density ratio: (a) dimensionless natural frequency, (b) dimensionless damping

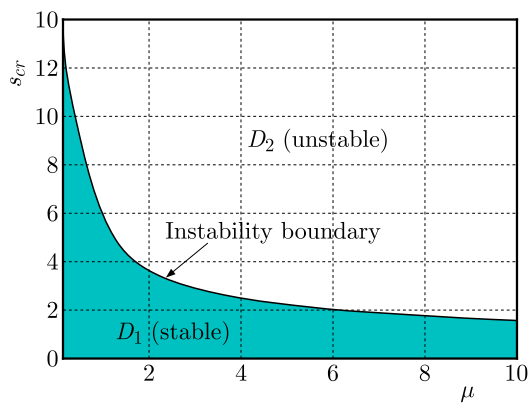


Fig. 11. Effects of the density ratio μ on the instability of the spinning shaft system

Moreover, the variations of critical spinning speeds for the considered spinning shaft versus the density ratio and slenderness ratio are presented in Fig. 12. In this figure, by increasing the

density ratio, the critical spinning speeds of the shaft decrease in each order. Also, by increasing the slenderness ratio, the critical spinning speeds change smoothly. In particular, the critical spinning speed approaches almost a constant value when the aspect ratio is sufficiently large.

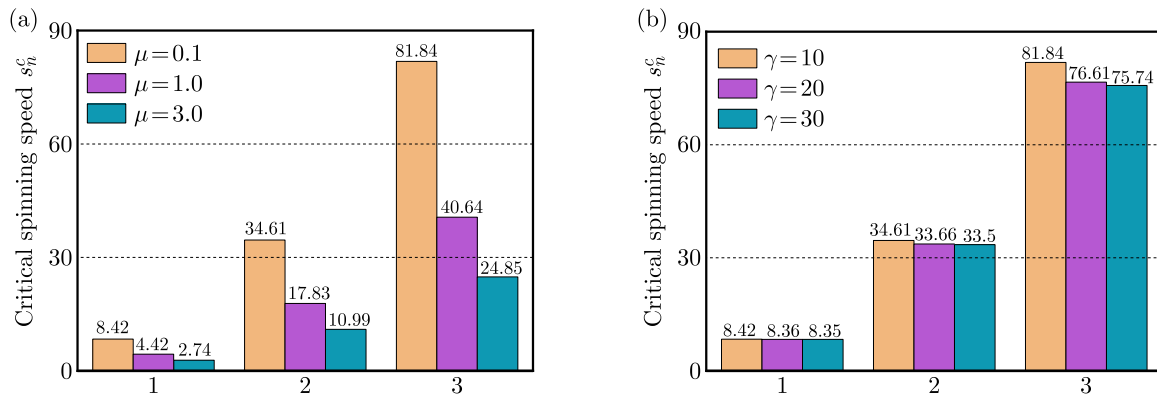


Fig. 12. Effects of main parameters on the critical spinning speed S_n^c : (a) density ratio μ , (b) slenderness ratio γ

5. Conclusions

In this study, stability of a spinning shaft in a concentric cylinder filled with an incompressible fluid has been theoretically addressed. The two-dimensional Navier-Stokes equations and continuity equation for the external fluid in the steady state were established, and the external fluid forces exerted on the shaft were calculated by using Taylor expansion. The governing equation of motion of the spinning shaft was formulated on the basis of Rayleigh beam theory. For pinned-pinned end supports, the explicit characteristic frequency equation has been derived analytically. The effects of slenderness ratio and density ratio on the natural frequencies and instability of the spinning shaft were investigated. The results showed that the critical spinning speed of each order for the system becomes smaller and the shape of the whirl speed map changed significantly due to the influence of the external fluid. Also, it was found that the shaft became unstable at a certain speed. This result indicated that the external fluid was the main source of the rotational shaft instability. Based on the present work, it could be concluded that the instability of the system is not very sensitive for a large slenderness ratio. However, the density ratio plays a determinant role in the natural frequency and stability of the system. It was shown that by increasing the density ratio, the natural frequency of the system was reduced and the stability became weaker. In addition, the results revealed that the external fluid had a significant effect on the critical spinning speed of the shaft. It was seen that as the density ratio increased, the critical speed value of the system decreased gradually.

Acknowledgments

The authors would like to acknowledge the financial support of the National Natural Science Foundation of China (No. 51775093), Natural Science Foundation of Anhui Province (2208085QE150), and University Natural Science Research Project of Anhui Province (No. KJ2021A0159) to this work.

References

1. ABDOLLAHI R., FIROUZ-ABADI R.D., RAHMANIAN M., 2021, On the stability of rotating pipes conveying fluid in annular liquid medium, *Journal of Sound and Vibration*, **494**, 115891
2. AOUDI M.A., LAKRAD F., 2018, On mathematical modelling of linear flexural vibrations of spinning Rayleigh beams, *Journal of Sound and Vibration*, **430**, 17-35

3. ARVIN H., 2019, On parametrically excited vibration and stability of beams with varying rotating speed, *Iranian Journal of Science and Technology-Transactions of Mechanical Engineering*, **43**, 2,177-185
4. BAHAAADINI R., DASHTBAYAZI M.R., HOSSEINI M., KHALILI-PARIZI Z., 2018, Stability analysis of composite thin-walled pipes conveying fluid, *Ocean Engineering*, **160**, 311-323
5. BAHAAADINI R., SAIDI A.R., 2018, Stability analysis of thin-walled spinning reinforced pipes conveying fluid in thermal environment, *European Journal of Mechanics; A/Solids*, **72**, 298-309
6. CHEN L.W., KU D.M., 1990, Dynamic stability analysis of a rotating shaft by the finite element method, *Journal of Sound and Vibration*, **143**, 1, 143-151
7. DWIVEDI A.R., DHIMAN A., SANYAL A., 2022, Stratified shear-thinning fluid flow past tandem cylinders in the presence of mixed convection heat transfer with a channel-confined configuration, *Journal of Fluids Engineering*, **144**, 5, 051301
8. EBRAHIMI-MAMAGHANI A., FOROOGHI A., SARPARAST H., ALIBEIGLOO A., FRISWELL M.I., 2021, Vibration of viscoelastic axially graded beams with simultaneous axial and spinning motions under an axial load, *Applied Mathematical Modelling*, **90**, 131-150
9. ELNAJJAR J., DANESHMAND F., 2020, Stability of horizontal and vertical pipes conveying fluid under the effects of additional point masses and springs, *Ocean Engineering*, **206**, 106943
10. FIROUZ-ABADI R.D., HADDADPOUR H., 2010, The flexural instability of spinning flexible cylinder partially filled with viscous liquid, *Journal of Applied Mechanics*, **77**, 1, 1001
11. GROSS P., GÜRGÖZE M., KLIEM W., 1993, Bifurcation and stability analysis of a rotating beam, *Quarterly of Applied Mathematics*, **51**, 4, 701-711
12. KATZ R., 2001, The dynamic response of a rotating shaft subject to an axially moving and rotating load, *Journal of Sound and Vibration*, **246**, 5, 757-775
13. KERN D., JEHL G., 2016, Dynamics of a rotor partially filled with a viscous incompressible fluid, *PAMM*, **16**, 1, 279-280
14. KHEIRI M., PAÏDOUSSIS M.P., DEL POZO G.C., AMABILI M., 2014, Dynamics of a pipe conveying fluid flexibly restrained at the ends, *Journal of Fluids and Structures*, **49**, 360-385
15. LI C., MIAO X., QIAO R., TANG Q., 2021, Modeling method of bolted joints with micro-slip features and its application in flanged cylindrical shell, *Thin-Walled Structures*, **164**, 107854
16. LI Q., 2022, New approach for bearing fault diagnosis based on fractional spatio-temporal sparse low rank matrix under multichannel time-varying speed condition, *IEEE Transactions on Instrumentation and Measurement*, **71**, 1-12
17. LI S.J., LIU G.M., KONG W.T., 2014, Vibration analysis of pipes conveying fluid by transfer matrix method, *Nuclear Engineering and Design*, **266**, 78-88
18. LI X., QIN Y., LI Y. H., ZHAO X., 2018, The coupled vibration characteristics of a spinning and axially moving composite thin-walled beam, *Mechanics of Advanced Materials and Structures*, **25**, 9, 722-731
19. LIANG F., GAO A., YANG X.D., 2020, Dynamical analysis of spinning functionally graded pipes conveying fluid with multiple spans, *Applied Mathematical Modelling*, **83**, 454-469
20. LIANG F., YANG X.D., QIAN Y.J., ZHANG W., 2018, Transverse free vibration and stability analysis of spinning pipes conveying fluid, *International Journal of Mechanical Sciences*, **137**, 195-204
21. MANCHI V., SUJATHA C., 2021, Torsional vibration reduction of rotating shafts for multiple orders using centrifugal double pendulum vibration absorber, *Applied Acoustics*, **174**, 107768
22. MICHAELIDES E.E., FENG Z.G., 2023, Drag coefficients of non-spherical and irregularly-shaped particles, *Journal of Fluids Engineering*, **145**, 6, 1-74

23. OYELADE A.O., OYEDIRAN A.A., 2020, Imperfect bifurcation and chaos of slightly curved carbon nanotube conveying hot pressurized fluid resting on foundations, *Journal of Fluids Engineering*, **142**, 11
24. PAÏDOUSSIS M.P., ISSID N.T., 1974, Dynamic stability of pipes conveying fluid, *Journal of Sound and Vibration*, **33**, 3, 267-294
25. QIAN Q., WANG L., NI Q., 2009, Instability of simply supported pipes conveying fluid under thermal loads, *Mechanics Research Communications*, **36**, 3, 413-417
26. SAEED N.A., 2019, On vibration behavior and motion bifurcation of a nonlinear asymmetric rotating shaft, *Archive of Applied Mechanics*, **89**, 9, 1899-1921
27. SAHEBNASAGH M., NIKKHAH-BAHRAMI M., FIROUZ-ABADI R.D., 2018, Effect of multiphase fluid and functionally graded density fluid on the stability of spinning partially-filled shells, *International Journal of Mechanical Sciences*, **140**, 109-118
28. SHAHGHOLI M., KHADEM S.E., BAB S., 2014, Free vibration analysis of a nonlinear slender rotating shaft with simply support conditions, *Mechanism and Machine Theory*, **82**, 128-140
29. SHEU G.J., YANG S.M., 2005, Dynamic analysis of a spinning Rayleigh beam, *International Journal of Mechanical Sciences*, **47**, 157-169
30. TAO M.D., ZHANG W., 2002, Dynamic stability of a flexible spinning cylinder partially filled with liquid, *Journal of Applied Mechanics*, **69**, 5, 708-710
31. WANG G.D., YUAN H.Q., 2018, An analysis of dynamic stability for a flexible rotor filled with liquid, *Physics of Fluids*, **30**, 3, 037101
32. WANG G., YUAN H., 2019a, Dynamic stability analysis of a flexible rotor filled with liquid based on three-dimensional flow, *Journal of Fluids Engineering*, **141**, 5
33. WANG G.D., YUAN H.Q., 2019b, Stability analysis of a flexible rotor partially filled with two liquid phases, *Physics of Fluids*, **31**, 017103
34. WANG G.D., YUAN H.Q., 2021, Dynamics and stability analysis of an axially functionally graded hollow rotor partially filled with liquid, *Composite Structures*, **266**, 113821
35. WANG H.F., CHEN C., 2020, Stability analysis of a rotor system with fluid applying wave resonance theory, *Physics of Fluids*, **32**, 5, 054106
36. WANG H.F., CHEN G., JIANG G.Y., 2021, Stability analysis of an anisotropic rotor partially filled with viscous incompressible fluid based on Andronov-Hopf bifurcation, *Physics of Fluids*, **33**, 6, 064111
37. YANG S., HU H., MO G., ZHANG X., QIN J., YIN S., ZHANG J., 2021, Dynamic modeling and analysis of an axially moving and spinning Rayleigh beam based on a time-varying element, *Applied Mathematical Modelling*, **95**, 409-434
38. ZHANG Y., YANG X., ZHANG W., 2020a, Modeling and stability analysis of a flexible rotor based on the Timoshenko beam theory, *Acta Mechanica Solida Sinica*, **33**, 3, 281-293
39. ZHANG J.W., ZHU L., CHEN P., WU Q.M., WEI M., YIN C.L., LI G.L., 2020b, Flowing interaction between cutting edge of ploughbreast with soil in shifting tillage operations, *Engineering Applications of Computational Fluid Mechanics*, **14**, 1, 1404-1415
40. ZHOU X.W., DAI H.L., WANG L., 2018, Dynamics of axially functionally graded cantilevered pipes conveying fluid, *Composite Structures*, **190**, 112-118
41. ZHU K., CHUNG J., 2019, Vibration and stability analysis of a simply-supported Rayleigh beam with spinning and axial motions, *Applied Mathematical Modelling*, **66**, 362-382
42. ZHU L., LUO F., QI Y.Y., WEI M., GE J.R., LIU W.L., LI G.L., JEN T.C., 2018, Effects of spray angle variation on mixing in a cold supersonic combustor with kerosene fuel, *Acta Astronautica*, **144**, 1-11